PROCEEDINGS OF SCIENCE

Precision $B^*B\pi$ coupling from three-flavor lattice QCD

Antoine Gérardin[a], **Jochen Heitger**[b], **Simon Kuberski**[c,d,*], **Hubert Simma**[e] **and Rainer Sommer**[e,f]

ALPHA Collaboration

[a] *Aix Marseille Univ, Université de Toulon, CNRS, CPT, Marseille, France*

[b] *Institut für Theoretische Physik, Westfälische Wilhelms-Universität Münster, Wilhelm-Klemm-Straße 9, 48149 Münster, Germany*

[c] *Helmholtz-Institut Mainz, Johannes Gutenberg-Universität Mainz, Staudingerweg 18, 55128 Mainz, Germany*

[d] *GSI Helmholtzzentrum für Schwerionenforschung, Planckstraße 1, 64291 Darmstadt, Germany*

[e] *John von Neumann Institute for Computing (NIC), DESY, Platanenallee 6, 15738 Zeuthen, Germany*

[f] *Institut für Physik, Humboldt-Universität zu Berlin, Newtonstraße 15, 12489 Berlin, Germany*

E-mail: simon.kuberski@uni-mainz.de

We consider three-flavor QCD and perform a determination of the low-energy coupling $\hat{g}_\chi$ of SU(2) Heavy Meson Chiral Perturbation Theory. It is the $B^*B\pi$ coupling in the limit of static heavy and chiral light quarks and has not been determined with precision thus far. The calculation is performed on a large set of the 2 + 1 flavor CLS ensembles with pion masses from 420 MeV down to 130 MeV. This allows us to significantly reduce the systematic uncertainty from the chiral extrapolation compared to previous works. Only a weak dependence on the lattice spacing is visible in our results.

MS-TP-21-31
MITP-21-052
DESY-21-176

The 38th International Symposium on Lattice Field Theory, LATTICE2021 26th-30th July, 2021 Zoom/Gather@Massachusetts Institute of Technology

*Speaker

PoS(LATTICE2021)540

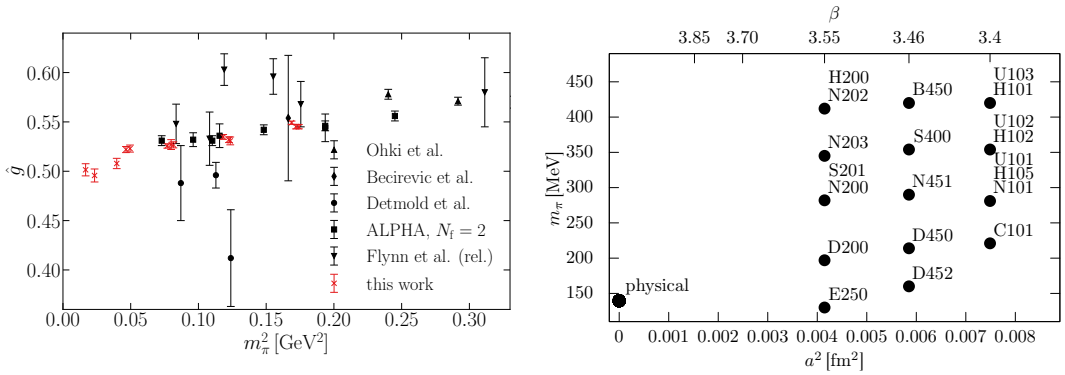

Figure 1: *Left:* Dependence of $\hat{g}$ on the pion mass. Comparison of this work (in red) with existing work based on dynamical light quarks in Refs. [3–7]. The results have been obtained at finite lattice spacing. *Right:* Overview of the ensembles used in this work in the landscape of squared lattice spacing and pion mass. The strange quark mass is implicitly fixed by the chiral trajectory. Multiple IDs at the same point indicate a variation of the spatial lattice size.

1. The $B^*B\pi$ coupling in the static approximation

The interactions of heavy-light mesons and soft pseudo-Goldstone bosons in Heavy Meson Chiral Perturbation Theory (HMχPT) at lowest order are governed by a single low-energy constant $\hat{g}_\chi$ [1]. This constant is related to the would-be matrix element of the strong decay $B^* \to B\pi$ which is kinematically forbidden in nature and therefore inaccessible from experiment. In contrast, it is possible to compute the coupling $\hat{g}$ on the lattice [2] from the matrix element of the light-light axial current,

$$\hat{g} = \frac{1}{2}\langle B^0(\mathbf{0})|\hat{A}_k(0)|B_k^{*\dagger}(\mathbf{0})\rangle\,, \tag{1}$$

in the limit of infinitely heavy b-quark mass. The calculation is performed using static heavy quarks and light quarks heavier than physical, followed by an extrapolation to vanishing light quark masses to obtain $\hat{g}_\chi$.

Amongst other applications, the precise knowledge of $\hat{g}_\chi$ is relevant to constrain chiral extrapolations of interesting B physics observables that are computed on the lattice. In existing work using dynamical light quarks, a significant systematic uncertainty is present due to a long chiral extrapolation from pion masses above 270 MeV. This is illustrated on the left hand side of figure 1 showing the results of Refs. [3–7] together with preliminary results of this work. In addition, systematic uncertainties due to excited-state contributions in the extraction of hadronic matrix elements require special attention in the analysis.

2. Computing $\hat{g}$ on the lattice

The extraction of matrix elements from lattice data is complicated by statistical errors that become significant for source-sink separations of O(1 fm) and systematic errors due to the contamination by excited states at small distances. In order to obtain a reliable estimate for the matrix elements, both sources of uncertainty have to be reduced simultaneously as much as possible. The

suppression of excited-state contaminations in the extraction of hadron-to-hadron transition matrix elements has been discussed in Ref. [8]. There, a combination of the summation method [9] with the solution of a Generalized Eigenvalue Problem (GEVP) [10–12] has been introduced and shown to minimize systematic uncertainties, when compared to the summation method or the GEVP alone.

The method is based on the computation of an $N \times N$ matrix of three-point functions

$$(D_{ij}^{3\mathrm{pt}})_k(t) = \sum_{t_1=0}^{T-1} \langle \left(B_i^*\right)_k(t) \, (A_\mathrm{R})_k(t_1) \, B_j^\dagger(0) \rangle \,, \tag{2}$$

summed over the insertion time t_1. The correlation functions are constructed out of a set of N interpolating operators, denoted by i, j in eq. (2). The index k indicates the spatial polarization of the axial current. Together with the summed three-point function, the corresponding matrix of two-point functions

$$C_{ij}^{2\mathrm{pt}}(t) = \langle B_i(t) B_j^\dagger(0) \rangle \tag{3}$$

is computed. The solution of a GEVP at time separations t and t_0,

$$C^{2\mathrm{pt}}(t) v_n(t, t_0) = \lambda_n(t, t_0) C^{2\mathrm{pt}}(t_0) v_n(t, t_0) \,, \tag{4}$$

gives access to the eigenvectors v_n and eigenvalues λ_n, corresponding to the energies of the low-lying states [12]. Following Ref. [8], these can be employed to extract effective matrix elements via

$$M_n^{\mathrm{eff}}(t, t_0) = -\frac{1}{2} \partial_t \frac{\left(v_n(t, t_0), \left[\frac{D^{3\mathrm{pt}}(t)}{\lambda_n(t, t_0)} - D^{3\mathrm{pt}}(t_0) \right] v_n(t, t_0) \right)}{\left(v_n(t, t_0), C^{2\mathrm{pt}}(t_0) v_n(t, t_0) \right)} = \hat{g}_{nn} + \mathrm{O}(e^{-(E_{N+1} - E_n)t}) \,. \tag{5}$$

The effective matrix element M_n^{eff} matches $\hat{g}_{nn}$ up to corrections that vanish exponentially with the source-sink separation and the energy gap $\Delta_{N,n} \equiv (E_{N+1} - E_n)$ for a GEVP of size N, provided that $t_0 \geq t/2$ is chosen. For the phenomenologically most relevant case of $n = 1$, $\hat{g} \equiv g_{11}$, excited states are suppressed with $\Delta_{N,1} > 1$ GeV for $N > 3$ in our calculation. The set of interpolating operators is constructed from smeared quark fields. We employ Gaussian smearing with APE-smeared gauge links [13–15], as well as smearing via three-dimensional scalar and spinor auxiliary fields [16], and test different combinations of operators in our variational basis. We note that it might be possible that the contamination by multi-hadron states, similar to those discussed in [17], is not entirely controlled by the used GEVP. Worries are the dense spectrum of multi-hadron states in large volume and insufficient overlaps with those states when using just local interpolating fields.

To improve the signal-to-noise-ratio, we employ time-diluted stochastic sources [18, 19] for the light quarks to profit from time-slice volume averaging. Three-point functions are obtained from sequential propagators. The use of HYP-smeared static quark actions [20, 21] reduces statistical fluctuations by a factor that grows exponentially with the time separation. We employ the HYP1 and HYP2 actions of Ref. [21] and obtain two sets of results that differ by $\mathrm{O}(a^2)$ effects.

2.1 Computational Setup

We perform our calculation at three resolutions on the $\mathrm{Tr}[M_\mathrm{q}] = \text{const.}$ trajectory of the $N_\mathrm{f} = 2 + 1$ CLS ensembles [22], generated with $\mathrm{O}(a)$ clover-improved Wilson quarks and tree-level

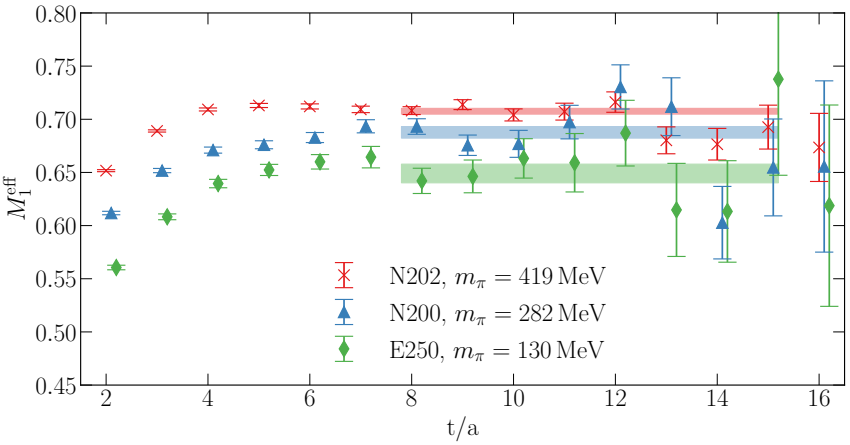

Figure 2: Representative extraction of the bare matrix elements M_1^{eff} at $a \approx 0.064$ fm at three different pion masses, including the SU(3) flavor symmetric point and close to physical quark masses.

improved Lüscher-Weisz gluons. An overview is given on the right hand side of figure 1. Ensembles with open and periodic boundary conditions in time direction enter our analysis. We cover a range of light quark masses that spans from the SU(3)-flavor-symmetric point, where $m_\pi = m_K \approx 420$ MeV, down to slightly smaller than physical light quark masses. The strange quark mass is fixed implicitly by our chiral trajectory. At five points in the (a^2, m_π) plane, we vary the spatial box sizes to explicitly test for finite-volume effects in our calculation.

Our quark action is O(a) improved using the determination of c_{SW} from Ref. [23]. The improvement and renormalization of the axial current that enters the effective matrix elements amounts to the renormalization pattern [24]

$$(M_{\text{R}}^{\text{eff}})_n = Z_{\text{A}}(1 + b_{\text{A}} am_{\text{q}} + \bar{b}_{\text{A}} a\text{Tr}\left[M_{\text{q}}\right])M_n^{\text{eff}} \,. \tag{6}$$

We employ the renormalization constant Z_{A} that has been determined to high precision in [25] and the improvement coefficients b_{A} and $\bar{b}_{\text{A}}$ from Refs. [26, 27]. The critical hopping parameters that enter the computation of the bare subtracted quark masses am_{q} have been obtained from Refs. [28, 29].

When solving the GEVP, we choose $t_0 = t/2$ to suppress excited-state contamination, cf. eq. (5). We determine the minimal time separation where excited state effects have sufficiently vanished by requiring

$$\left|M_n^{\text{eff}}(t) - M_n^{\text{eff}}(t - \delta t)\right| < \sigma(t) \tag{7}$$

where $\delta t = \frac{1}{\Delta_{N,n}}$ is extracted from the GEVP via $\lambda_n(t)$ and $\sigma(t)$ are the statistical errors on $M_n^{\text{eff}}(t)$. We find that the criterion of eq. (7) is fulfilled for $t \geq 0.5$ fm on all of our ensembles. To avoid a propagation of statistical fluctuations at single source-sink separations on some ensembles into the plateau averages, we fix $t_{\text{min}} = 0.52$ fm for all ensembles. In a later stage of our analysis, we verify that a variation of t_{min} in a range $[0.3\,\text{fm}, 0.9\,\text{fm}]$ does not have a significant influence on the result in the chiral-continuum limit, albeit with large statistical uncertainties for t_{min} as large as 0.9 fm. We set the upper end of the plateau range to the time slice where the relative error

on $M_n^{\text{eff}}(t)$ exceeds 30 %, which is the case at about 1 fm for the summed GEVP across all of our ensembles. In figure 2, we illustrate plateau fits at our finest lattice spacing at three different pion masses, including the physical one. It is visible that the signal deteriorates quickly. However, we are able to identify reasonable plateaus.

3. Extrapolation to the chiral-continuum limit

To arrive at $\hat{g}_\chi$, we have to extrapolate to the infinite volume, continuum and chiral limits. Our parametrization for the combined extrapolation is based on Ref. [30] and reads

$$\begin{aligned} \hat{g}_{11} \equiv \hat{g}_\chi \Big[& 1 - (1 + 2\hat{g}_\chi^2)\, y \log y + c_1 y + c_2 y^2 + \dots && \textit{chiral dependence} \\ & + \hat{g}_\chi^2\, y\, F_0(m_\pi L) + y\, F_1(m_\pi L) + \dots && \textit{finite-volume effects} \\ & + c_a a^2 + \dots \Big] && \textit{cutoff effects}, \\ \text{with} \quad & F_n(z) = \mathrm{O}\left(\mathrm{e}^{-z} z^{-1/2-n}\right), \end{aligned} \tag{8}$$

where the dependence on the pion mass is parametrized via $y \equiv \frac{m_\pi^2}{8\pi^2 f_\pi^2}$. A leading logarithmic dependence on y is predicted from chiral perturbation theory and complicates the extrapolation from larger-than-physical pion masses to the chiral limit. The exact form of the leading finite-volume effects based on chiral perturbation theory has been derived in Ref. [30]. Since we work with $m_\pi L \gtrsim 4$, these effects are small: The leading χPT expression predicts a relative deviation of 0.5% at the symmetric point and sub per mill effects at physical pion mass for $m_\pi L = 4$. Due to the non-perturbative $\mathrm{O}(a)$ improvement of action and currents, the leading cutoff effects are of $\mathrm{O}(a^2)$.

We carry out a combined fit to extract $\hat{g}_\chi$ as our estimate for the (infinite-volume) LEC of HMχPT. Figure 3 illustrates an exemplary fit to the renormalized effective matrix elements. We show the results at finite lattice spacing together with the fit function, evaluated at all three resolutions (colored lines), as well as the functional form in the continuum limit. Here, the statistical uncertainty is depicted by the gray band. The inclusion of a term proportional to y^2 allows us to describe the data in the complete range of pion masses. Despite the inclusion of results close to physical pion masses, it is hard to constrain the chiral limit due to the presence of the logarithmic term in the extrapolation. However, for the first time, a deviation from a linear behavior in y towards the chiral limit is visible in our data. The systematic uncertainty due to the chiral extrapolation, which has to be included in our final results, will be estimated based on a variation of the functional form and cuts on the maximal pion mass.

Cutoff effects appear to be small for both static quark discretizations. Nevertheless, we are able to resolve a dependence on a^2 for both actions. Our continuum extrapolations of results based on HYP1 and HYP2 actions coincide with each other and with a combined extrapolation of the two sets. The data is compatible with cutoff effects proportional to a^2 without a mass-dependence.

We adopt and compare different strategies for the description of finite-volume effects. Based on the ensembles with reduced box sizes, which are shown in figure 1, we are able to compare the expectation from chiral perturbation theory with our data and to include the observed deviations

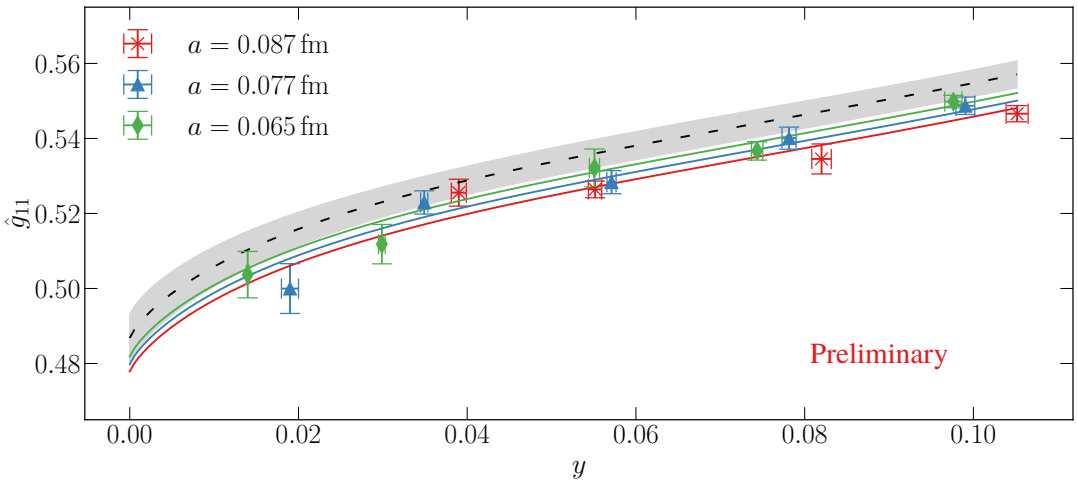

Figure 3: Illustration of a preliminary combined chiral and continuum extrapolation. Results at three lattice spacings enter the fit, as indicated by different colors. The corresponding lines show the quark mass dependence at those lattice spacings, as determined by the fit. The gray band gives the uncertainty on the quark mass dependence in the continuum limit. We show results using the HYP2 action for the static quarks.

in our fits. In figure 4 we illustrate the renormalized effective matrix elements as determined from plateau fits at two different pion masses and $a \approx 0.087\,\mathrm{fm}$. Together with the data, we show the NLO prediction based on chiral perturbation theory. It is apparent that this prediction is not able to describe the deviations from the infinite-volume limit at small values of $m_\pi L$. However, these effects appear to be small for the larger boxes. For comparison, we also show the result of a fit to the finite-volume effects, which is obtained by including the small volumes in a combined chiral-continuum-volume extrapolation. For this fit, we add a fit parameter c_{FV} to the analytical form,

$$\hat{g}_{11}^{\mathrm{FV}} = \hat{g}_\chi \left[1 + \hat{g}_\chi^2\, y\, F_0(m_\pi L) + c_{\mathrm{FV}}\, y\, F_1(m_\pi L)\right] , \tag{9}$$

where $c_{\mathrm{FV}} = 1$ in χPT. We are able to describe the data at small $m_\pi L$ with the fit result. At large $m_\pi L$, the deviation from the χPT prediction is small. Consequently, the extrapolated result does not change significantly, when we switch between the two descriptions, or even neglect finite-volume effects at all.

4. Conclusions

We will be able to determine $\hat{g}_\chi$ with much improved precision and better controlled systematics compared to existing work. We employ a number of well-established techniques, such as the use of random sources and the summed GEVP to extend the window where an extraction of matrix elements is possible without the introduction of large statistical and systematic uncertainties. The main improvement of our calculation with respect to existing work is the inclusion of a number of ensembles at pion masses below 270 MeV down to 130 MeV. This allows us to constrain the chiral extrapolation more tightly and to reduce the leading systematic uncertainty that was present in the

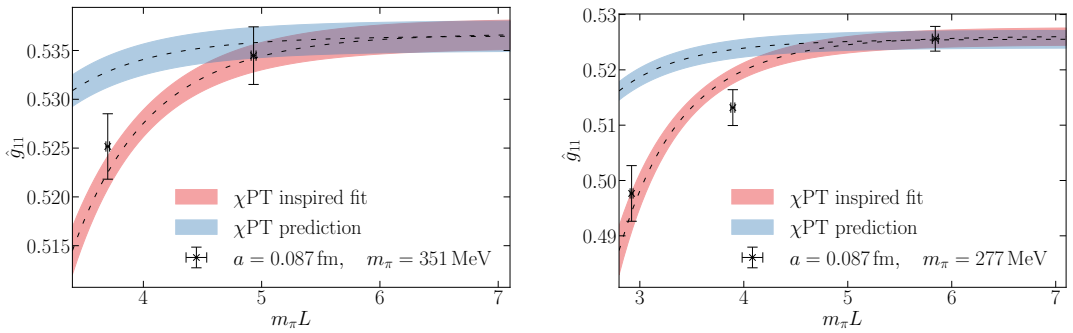

Figure 4: Finite-volume effects for two different pion masses at the coarsest lattice spacing in our analysis. We show a comparison of fit results using a free fit parameter c_{FV} and using $c_{\mathrm{FV}} = 1$ in the combined chiral, continuum and finite-volume extrapolation.

so far most precise lattice calculation of Ref. [6]. The final assessment of the remaining systematic uncertainty is not yet finished and will be addressed in the forthcoming publication [31]. The knowledge of $\hat{g}_\chi$ will help us to perform chiral extrapolations of phenomenologically interesting quantities in the ALPHA program for B physics with $2 + 1$ flavors of light quarks [32–34].

Acknowledgements

The work of JH and SK has been supported by the Deutsche Forschungsgemeinschaft (DFG) through the Research Training Group *GRK 2149: Strong and Weak Interactions – from Hadrons to Dark Matter*. This publication received funding from the Excellence Initiative of Aix-Marseille University – A*MIDEX, a French "Investissements d'Avenir" programme, AMX-18-ACE-005. The authors gratefully acknowledge the Gauss Centre for Supercomputing e.V. (www.gauss-centre.eu) for funding this project by providing computing time on the GCS Supercomputer SuperMUC-NG at Leibniz Supercomputing Centre (www.lrz.de). We furthermore acknowledge the computer resources provided by the WWU IT of the University of Münster (PALMA-II HPC cluster) and by DESY Zeuthen (PAX cluster) and thank the staff of the computing centers for their support. We are grateful to our colleagues in the CLS initiative for producing the gauge field configuration ensembles used in this study.

References

[1] R. Casalbuoni, A. Deandrea, N. Di Bartolomeo, R. Gatto, F. Feruglio and G. Nardulli, *Phenomenology of heavy meson chiral Lagrangians*, *Phys. Rept.* **281** (1997) 145 [hep-ph/9605342].

[2] G.M. de Divitiis, L. Del Debbio, M. Di Pierro, J.M. Flynn, C. Michael and J. Peisa, *Towards a lattice determination of the $B^*B\pi$ coupling*, *JHEP* **10** (1998) 010 [hep-lat/9807032].

[3] H. Ohki, H. Matsufuru and T. Onogi, *Determination of $B^*B\pi$ coupling in unquenched QCD*, *Phys. Rev. D* **77** (2008) 094509 [0802.1563].

[4] D. Becirevic, B. Blossier, E. Chang and B. Haas, *$g_{B^*B\pi}$-coupling in the static heavy quark limit*, *Phys. Lett. B* **679** (2009) 231 [0905.3355].

[5] W. Detmold, C.J.D. Lin and S. Meinel, *Calculation of the heavy-hadron axial couplings g_1, g_2 and g_3 using lattice QCD*, *Phys. Rev. D* **85** (2012) 114508 [1203.3378].

[6] F. Bernardoni, J. Bulava, M. Donnellan and R. Sommer, *Precision lattice QCD computation of the $B^*B\pi$ coupling*, *Phys. Lett. B* **740** (2015) 278 [1404.6951].

[7] J.M. Flynn, P. Fritzsch, T. Kawanai, C. Lehner, B. Samways, C.T. Sachrajda et al., *The $B^*B\pi$ Coupling Using Relativistic Heavy Quarks*, *Phys. Rev. D* **93** (2016) 014510 [1506.06413].

[8] J. Bulava, M. Donnellan and R. Sommer, *On the computation of hadron-to-hadron transition matrix elements in lattice QCD*, *JHEP* **01** (2012) 140 [1108.3774].

[9] L. Maiani, G. Martinelli, M.L. Paciello and B. Taglienti, *Scalar Densities and Baryon Mass Differences in Lattice QCD with Wilson Fermions*, *Nucl. Phys. B* **293** (1987) 420.

[10] C. Michael, *Adjoint Sources in Lattice Gauge Theory*, *Nucl. Phys.* **B259** (1985) 58.

[11] M. Lüscher and U. Wolff, *How to Calculate the Elastic Scattering Matrix in Two-dimensional Quantum Field Theories by Numerical Simulation*, *Nucl. Phys.* **B339** (1990) 222.

[12] B. Blossier, M. Della Morte, G. von Hippel, T. Mendes and R. Sommer, *On the generalized eigenvalue method for energies and matrix elements in lattice field theory*, *JHEP* **04** (2009) 094 [0902.1265].

[13] S. Güsken, U. Löw, K.H. Mütter, R. Sommer, A. Patel and K. Schilling, *Nonsinglet Axial Vector Couplings of the Baryon Octet in Lattice QCD*, *Phys. Lett.* **B227** (1989) 266.

[14] M. Albanese et al., *Glueball Masses and String Tension in Lattice QCD*, *Phys. Lett. B* **192** (1987) 163.

[15] S. Basak, I. Sato, S. Wallace, R. Edwards, D. Richards, G.T. Fleming et al., *Combining quark and link smearing to improve extended baryon operators*, *PoS* **LAT2005** (2006) 076 [hep-lat/0509179].

[16] M. Papinutto, F. Scardino and S. Schaefer, *New extended interpolating fields built from three-dimensional fermions*, *Phys. Rev. D* **98** (2018) 094506 [1807.08714].

[17] O. Bär, *$N\pi$-state contamination in lattice calculations of the nucleon axial form factors*, *Phys. Rev. D* **99** (2019) 054506 [1812.09191].

[18] R. Sommer, *Leptonic decays of B and D mesons*, *Nucl. Phys. B Proc. Suppl.* **42** (1995) 186 [hep-lat/9411024].

[19] J. Foley, K. Jimmy Juge, A. Ó Cais, M. Peardon, S.M. Ryan and J.-I. Skullerud, *Practical all-to-all propagators for lattice QCD*, *Comput. Phys. Commun.* **172** (2005) 145 [hep-lat/0505023].

[20] M. Della Morte, S. Dürr, J. Heitger, H. Molke, J. Rolf, A. Shindler et al., *Lattice HQET with exponentially improved statistical precision*, *Phys. Lett. B* **581** (2004) 93 [hep-lat/0307021].

[21] M. Della Morte, A. Shindler and R. Sommer, *On lattice actions for static quarks*, *JHEP* **08** (2005) 051 [hep-lat/0506008].

[22] M. Bruno et al., *Simulation of QCD with $N_f = 2 + 1$ flavors of non-perturbatively improved Wilson fermions*, *JHEP* **02** (2015) 043 [1411.3982].

[23] J. Bulava and S. Schaefer, *Improvement of $N_f = 3$ lattice QCD with Wilson fermions and tree-level improved gauge action*, *Nucl. Phys. B* **874** (2013) 188 [1304.7093].

[24] T. Bhattacharya, R. Gupta, W. Lee, S.R. Sharpe and J.M.S. Wu, *Improved bilinears in lattice QCD with non-degenerate quarks*, *Phys. Rev.* **D73** (2006) 034504 [hep-lat/0511014].

[25] M. Dalla Brida, T. Korzec, S. Sint and P. Vilaseca, *High precision renormalization of the flavour non-singlet Noether currents in lattice QCD with Wilson quarks*, *Eur. Phys. J. C* **79** (2019) 23 [1808.09236].

[26] G.S. Bali, V. Braun, S. Collins, A. Schäfer and J. Simeth, *Masses and decay constants of the η and η' mesons from lattice QCD*, *JHEP* **08** (2021) 137 [2106.05398].

[27] G.S. Bali et al., to appear.

[28] G.S. Bali, E.E. Scholz, J. Simeth and W. Söldner, *Lattice simulations with $N_f = 2 + 1$ improved Wilson fermions at a fixed strange quark mass*, *Phys. Rev. D* **94** (2016) 074501 [1606.09039].

[29] A. Gérardin, T. Harris and H.B. Meyer, *Nonperturbative renormalization and $O(a)$-improvement of the nonsinglet vector current with $N_f = 2 + 1$ Wilson fermions and tree-level Symanzik improved gauge action*, *Phys. Rev. D* **99** (2019) 014519 [1811.08209].

[30] W. Detmold, C.J.D. Lin and S. Meinel, *Axial couplings in heavy hadron chiral perturbation theory at the next-to-leading order*, *Phys. Rev. D* **84** (2011) 094502 [1108.5594].

[31] A. Gérardin, J. Heitger and S. Kuberski, *The static $B^*B\pi$ coupling of three flavor QCD*, in preparation.

[32] J. Heitger and R. Sommer, *Nonperturbative heavy quark effective theory*, *JHEP* **02** (2004) 022 [hep-lat/0310035].

[33] M. Della Morte, S. Dooling, J. Heitger, D. Hesse and H. Simma, *Matching of heavy-light flavour currents between HQET at order 1/m and QCD: I. Strategy and tree-level study*, *JHEP* **05** (2014) 060 [1312.1566].

[34] P. Fritzsch, J. Heitger and S. Kuberski, *$O(a)$ improved quark mass renormalization for a non-perturbative matching of HQET to three-flavor QCD*, *PoS* **LATTICE2018** (2018) 218 [1811.02591].